

# Whispering-gallery-mode biosensing: label-free detection down to single molecules

Frank Vollmer<sup>1</sup> & Stephen Arnold<sup>2</sup>

**Optical label-free detectors, such as the venerable surface plasmon resonance (SPR) sensor, are generally favored for their ability to obtain quantitative data on intermolecular binding. However, before the recent introduction of resonant microcavities that use whispering gallery mode (WGM) recirculation, sensitivity to single binding events had not materialized. Here we describe the enhancement mechanisms responsible for the extreme sensitivity of the WGM biosensor, review its current implementations and applications, and discuss its future possibilities.**

Biosensors that are label-free, miniature and ultrasensitive have been a dream of scientists and biotechnologists. Labels can structurally and functionally interfere with an assay, may not be specific and may be difficult to conjugate—a problem often encountered in single-molecule experiments. Without the need for labels, detection can be done on site and in real time, an important advantage in emerging point-of-care testing applications. In addition, the fidelity with which multiplexed label-free sensors follow receptor-analyte interactions in real time can improve quality and throughput in drug discovery<sup>1</sup>. Here we briefly present the primary mechanism by which traditional guided-wave label-free sensors operate and describe the WGM biosensor, a miniature optical device that recirculates a guided wave to enhance sensitivity down to a single molecule.

It is well known that light can be confined in a transparent material (for example, glass in aqueous buffer) if the angle at which it impacts the outer edge is less than a specific angle defined by the refractive index of the transmitting material and the outside, an effect known as total internal reflection. As this light is reflected, it induces an evanescent wave in the surrounding medium that propagates tangent to the surface and extends ~200 nm outward. This wave is commonly used to detect fluorophore-labeled proteins by stimulating fluorescence

emission that is subsequently detected by a microscope. Less well known is that the binding of polarizable molecules to the surface of a light guide can interact with this evanescent wave and slightly increase the path length and number of wavelengths of light through the guide (optical path length). Although this 'reactive' effect presents a means for unlabeled detection by interferometry, it is so weak for individual proteins that the ability to detect a single protein (for example, an antigen binding to a previously immobilized antibody) by resolving the accompanying phase change in interferometry is all but hopeless. The problem is that a given photon in the light guide interacts only once with an adsorbate. This is also true of the widely used SPR sensor<sup>2</sup>.

In 2002 we demonstrated a device<sup>3</sup> in which each photon guided by total internal reflection in a silica sphere (radius of ~100  $\mu\text{m}$ ) is recirculated many times, thereby providing a mechanism for increasing sensitivity<sup>4</sup>. Although the optical path length change along the circumference owing to binding of molecules works by the same 'reactive' effect as in a single-pass device, the added sensitivity arises from the precision with which this change can be measured. This enhanced precision is a consequence of resonance. Resonance occurs when the guided wave drives itself coherently by returning in phase after every revolution (Fig. 1), thereby requiring an integer number of waves in one circumnavigation. Light tuned into the driving fiber (Fig. 1b) reveals this condition as a dip at the resonance wavelength,  $\lambda_r$ , in the transmission spectrum (Fig. 1a). The binding of molecules increases the optical path length of the photon orbit, perturbing the sphere out of resonance. Getting the sphere back into resonance requires compensating for the binding events by increasing the wavelength of the driving laser by 'resonance shift',  $\Delta\lambda_r$  (Fig. 1a). Clearly this shift will not be observed unless it is comparable to or larger than the resonance linewidth,  $\delta\lambda_r$  (Fig. 1a). This is where resonance theory has its greatest role in enhancing detection sensitivity. As a general principle of

<sup>1</sup>The Rowland Institute, Harvard University, 100 Edwin H. Land Blvd., Cambridge, Massachusetts 02142, USA. <sup>2</sup>MicroParticle PhotoPhysics Lab (MP<sup>3</sup>L), Polytechnic University, 6 Metrotech Center, Brooklyn, New York 11201, USA. Correspondence should be addressed to S.A. (arnold@photon.poly.edu).

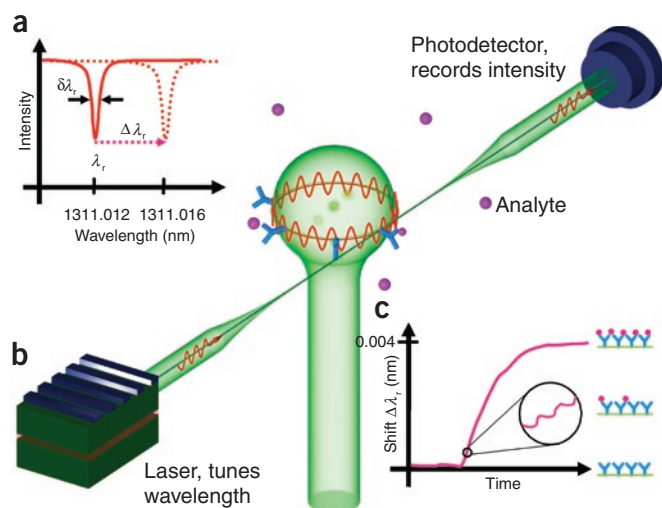


**Figure 1** | Concept of the WGM biosensor. (a) Resonance is identified at a specific wavelength from a dip in the transmission spectrum acquired with a tunable laser. The resonance wavelength,  $\lambda_r$ , is measured by locating the minimum of the transmission dip within its linewidth (arrows). A resonance shift associated with molecular binding,  $\Delta\lambda_r$ , is indicated by the dashed arrow. (b) WGM in a dielectric sphere driven by evanescent coupling to a tapered optical fiber<sup>3</sup>. The light wave (red) circumnavigates the surface of the glass sphere (green) where binding of analyte molecules (purple) to immobilized antibodies (blue) is detected from a shift of the resonance wavelength. (c) Binding of analyte is identified from a shift  $\Delta\lambda_r$  of resonance wavelength (also see a). Single-molecule binding is theorized to appear for the 'reactive' effect in the form of steps in the wavelength shift signal<sup>4</sup> (magnified inset). For microtoroid experiments using a 'thermo-optic' effect such steps have already been reported<sup>5</sup>.

all resonating systems, the resonance linewidth is inversely proportional to the energy decay time after the termination of the driving source. This decay time translates for the microsphere to the lifetime of the average photon. Consequently, the sensitivity with which a shift can be measured is proportional to the number of recirculations, which for our system is several thousand.

From the beginning, that sensitivity of the WGM approach for sensing the 'reactive' effect exceeded that of the SPR device. Since then ~100 papers have been published using our approach for many applications. But even with the enhanced sensitivity the resulting shift in resonance wavelength induced by a single molecule was very difficult to detect. Researchers achieved such ultimate sensitivity in 2007 using a silica micro-toroid instead of a microsphere to recirculate the light, and they easily reached single-molecule sensitivity by increasing the wavelength shift with a 'thermo-optic boost'<sup>5</sup>. The amplification of the shift was large enough to demonstrate detection of individual IL-2 protein from steps in the signal generated by cytokines binding to antibodies previously immobilized on the toroid surface. The reported sensitivity ( $10^{-16}$  M IL-2)<sup>5</sup> for the thermo-optic WGM technique exceeded that of even the most sensitive enzyme-linked immunosorbent assay (ELISA). Both the microsphere and microtoroid are known as WGM biosensors because they involve light that is guided in a similar way as the whisper heard by Lord Rayleigh from across the dome of St. Paul's cathedral. Below we will briefly describe the operation of the WGM technology and its current and possible future applications to biomolecular science and engineering.

## Whispering-gallery mode technology

An optical WGM may be represented by a light wave that circumnavigates near the surface of a glass sphere with a radius of ~100  $\mu\text{m}$  and returns back upon itself in phase. It is resonantly stimulated by evanescent coupling to a light guide<sup>6</sup> (for example, tapered optical fiber<sup>7</sup>; **Fig. 1b**), which is driven in turn by a laser at wavelength  $\lambda$ . Resonance is achieved by tuning the laser to a wavelength  $\lambda_r$  for which the microsphere circumference is an integer multiple of orbital wavelengths. This closure relation forces the resonance wavelength to change for the slightest change in microsphere radius,  $R$ , or orbital refractive index of the sphere,  $n$ , according to  $\Delta\lambda_r/\lambda_r = \Delta R/R + \Delta n/n$ . This relationship provides the sensing principle for a layer of protein (**Fig. 2** and **Box 1**). The tapered fiber not only serves to drive the resonance but also leads to a means for detecting the wavelength shift<sup>4</sup>. As the laser wavelength is tuned through  $\lambda_r$ , power is extracted from the fiber, causing a dip in the light transmitted to the detector<sup>8</sup> (**Fig. 1a**). Another advantage of fiber excitation is that it allows for small arrays to be built simply by having multiple microspheres of different sizes and antibodies coupled to the same fiber<sup>9</sup>.

A spectroscopist working in the biomedical area is likely to be surprised by the narrowness of the resonance dip in **Figure 1a** ( $\delta\lambda_r = \sim 0.0006$  nm). In comparison to line widths in molecular fluorescence or absorption spectroscopy at room temperature (~10 nm), it is extremely narrow, but in the field of WGM spectroscopy it is actually fairly broad. The narrowness of a linewidth,  $\delta\lambda_r$ , and the sensor performance are characterized by the resonator's quality factor,  $Q = \lambda_r/\delta\lambda_r$ . As the sensor detection limit is set by how well one can locate  $\lambda_r$ , a high  $Q$  is essential to resolve a small  $\Delta\lambda_r$  associated with the binding of a few molecules. Not too surprisingly,  $Q$  can be shown to be proportional to the number of recirculations by a photon. For the resonator depicted in **Figure 1b**,  $Q$  is limited to  $2 \times 10^6$  by the optical absorption of water near 1,300 nm. As one can locate a resonance to  $\delta\lambda_r/100$  with ease, one can measure a shift in a resonance for the example shown in **Figure 1a** down to 6 fm. A shift of this magnitude requires only a very thin layer of bound material.

A convenient coincidence for optical biosensors is that the dielectric properties of silica and the bound protein layer are similar. As a consequence, the optical effect of binding a compact monolayer of protein of thickness  $\Delta R$  is to increase the average radius of the sphere (**Fig. 2**). Because the resonance wavelength is proportional to the radius, the fractional shift in the wavelength is equal to the

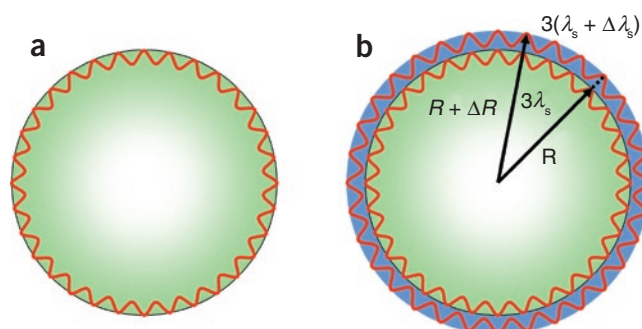


**Figure 2** | Model for estimating WGM biosensor layer sensitivity. (a) Bare sphere supporting a WGM. (b) WGM after the addition of a layer of thickness  $\Delta R$ . The geometry shows that the wavelength increases in proportion to the increase in radius (that is,  $\Delta\lambda_s/\lambda_s = \Delta R/R$ ).

## BOX 1 THEORY FOR WGM WAVELENGTH SHIFT OWING TO BIOMOLECULE BINDING

The way in which WGM changes when it reactively interacts with a bound protein molecule on the surface of a silica microsphere is currently not precisely understood. Our own calculations indicate that as a consequence of the binding event, the optical wave function protrudes further outward as the light passes the binding site thereby increasing the optical path length in an orbit. As more bound protein accumulates, so that the inter-protein separation is much less than the optical wavelength, an optically contiguous layer eventually forms with the protrusions merging, and the wave function simply follows a circular orbit but with a larger radius. At the maximum monolayer density the dielectric properties of condensed protein and silica are similar. In optical terms it is as if the silica sphere had grown by the thickness of the protein layer. In this limit and with this picture in mind, it is relatively easy to estimate the reactive resonance shift.

**Figure 2a** depicts a light wave circumnavigating a microsphere of radius  $R$  and returning in phase. The resonance condition is  $m\lambda_r/n = 2\pi R$ , where  $n$  is the orbital refractive index of the sphere, and  $m$  is the integer number of orbital wavelengths  $\lambda_s = \lambda_r/n$ . Based on this resonance condition the sensitivity of the resonance wavelength to changes in radius  $\Delta R$  or refractive index  $\Delta n$  is  $\Delta\lambda_r/\lambda_r = \Delta R/R + \Delta n/n$ . Increases in the radius or refractive index lead to a red shift in the WGM. With only the radius enlarged, an orbit having the same number of wavelengths must have its wavelength increased in proportion to the increase in radius:  $\Delta\lambda_r/\lambda_r = \Delta R/R$ . This simple idea was the basis for earlier thoughts on reactive WGM biosensing<sup>35</sup>. For a 1-nm protein monolayer bound on a 100  $\mu\text{m}$  sphere, the shift  $\Delta\lambda_r/\lambda_r$  is  $\sim 10^{-5}$ , which is 10,000 times our current noise level.

The results arrived at from our heuristic picture (**Fig. 2**) agree with Maxwell's equations for the case in which the layer has the same refractive index as the underlying sphere. Considering random coverage by a dilute layer of bioparticles requires an electromagnetic approach. Here each bioparticle binding to the surface shifts the resonance as a reaction to being polarized by the evanescent field. Consequently, the shift resulting from this 'reactive' effect is proportional to the excess polarizability,  $\alpha_{\text{ex}}$ , of each protein binding to the surface and to the average surface density,  $\sigma$ . The proportionality to polarizability adds an additional dimension to the WGM sensor over labeling techniques, as polarizability is proportional to the protein molecular weight. Overall<sup>4</sup>,

$$\frac{\Delta\lambda_r}{\lambda_r} = \frac{\alpha_{\text{ex}}\sigma}{\epsilon_0(n_s^2 - n_m^2)R} \quad (1)$$

where  $n_s$  and  $n_m$  are the refractive indices of the sphere and exterior medium, respectively. Note that the magnitude of the shift increases as the radius of the sphere decreases.

The reader may be surprised that although the key to the WGM enhancement is based on the number of recirculations of a photon in the mode, no parameter in equation 1 explicitly depends on the photon lifetime. That is because equation 1 describes only the shift and not the limit of detection (LOD). The lowest surface density that can be detected for a given WGM system depends on the resonance line width  $\delta\lambda_r$ , which in turn

is controlled by the  $Q$ ;  $\delta\lambda_r = \lambda_r/Q$ .  $Q$  is key to understanding the recirculation dependence because time domain analysis shows that  $Q$  is proportional to the average time a photon circulates in a mode; photon lifetime  $\tau = Q/\omega$ , where  $\omega$  is the resonance frequency. Furthermore, the limit of detection is not simply associated with having a shift equal to the linewidth,  $\delta\lambda_r$ , as a shift of only a fraction,  $F$ , of  $\delta\lambda_r$  can be sensed;  $(\Delta\lambda_r)_{\text{min}} = F\lambda_r/Q$ . On this basis the limit of detection of surface density is<sup>10</sup>

$$\sigma_{\text{LOD}} = \frac{R(n_s^2 - n_m^2)F}{(\alpha_{\text{ex}}/\epsilon_0)Q} \quad (2)$$

For the highest sensitivity one must minimize  $R/Q$ . Unfortunately  $R$  and  $Q$  are not independent, as reducing  $R$  ultimately leads to a decrease in  $Q$  owing to diffraction as well as other size-dependent losses. For a silica sphere in aqueous buffer near  $\lambda_r$  of  $\sim 780$  nm the minimum  $\sigma_{\text{LOD}}$  is reached for  $R$  of  $\sim 45$   $\mu\text{m}$ . With  $F = 0.01$ ,  $\sigma_{\text{LOD}}$  is about 0.03 pg/mm<sup>2</sup> for protein, which is nearly two orders of magnitude below the best  $\sigma_{\text{LOD}}$  reported for SPR. At this  $\sigma_{\text{LOD}}$  only  $9 \times 10^{-16}$  g needs to adsorb uniformly on the sphere to be detected. This is just a little more than the mass of an HIV ( $8 \times 10^{-16}$  g)<sup>10</sup>. Of course, most of the sphere's surface is insensitive to adsorption, so it would make more sense to place antibodies just at the equator where the principal energy circulates. For this condition the limit of mass detection for a single antigen binding to such an antibody is  $3.6 \times 10^{-17}$  g; less than 1/20 of an HIV mass<sup>10</sup>.

The detection of single molecular binding events based on the 'reactive' interaction has not yet been demonstrated by equatorial functionalization, but statistical fluctuations in the resonance frequency owing to diffusing virus-sized particles have been reported, and their autocorrelation agrees with the 'reactive' theory<sup>17</sup>. The first demonstration of single-molecule detection, however, is based on a slightly different interaction<sup>5</sup>.

Interaction between the oscillating evanescent field and a bioparticle at the sphere's surface not only polarizes the particle reactively (that is, in phase with the field), but also can absorb optical energy from the out-of-phase component. With nonradiative relaxation, a nanoscopic heat source is generated at the surface of the microsphere. Heating the sphere causes an additional resonance wavelength shift resulting from the 'thermo-optic' effect. As the sphere is warmed, its temperature increases locally, and its refractive index changes. If  $dn/dT$  is positive, as it is in silica, the refractive index will increase, and the resonance will shift toward the red in proportion to the circulating power,  $P$ . So unlike the reactive mechanism for which the wavelength shift sensitivity is independent of power, the thermo-optic mechanism affords a boost in sensitivity by increasing the power in the fiber,  $P_f$  (that is,  $P$  is proportional to  $P_f$ ). This boost is proportional to the resonant  $Q$ . Experiments with a micro-toroid have shown exceedingly high  $Q$  near  $3 \times 10^8$ , which translates into 100 W circulating in the resonator even though only 1 mW is launched into the fiber. As a result the shift is enhanced by orders of magnitude relative to the reactive effect.



fractional change in the radius:  $\delta\lambda_r/\lambda_r = \Delta R/R$ . Consequently, the minimum detectable thickness corresponding to a wavelength shift of 6 fm is  $\Delta R_{\min} = \sim 0.5$  pm (for  $R = 100$   $\mu\text{m}$  and  $\lambda_r = 1,300$  nm). As the size of a typical protein molecule is  $\sim 1$ – $10$  nm, our estimate for  $\Delta R_{\min}$  implies that an extremely small fraction of a monolayer should be detectable. Indeed, for nonideal parameters (that is, much larger microsphere,  $R = 200$   $\mu\text{m}$ ) we were able to detect as little as less than 1/1,000 of a monolayer of bovine serum albumin (BSA) in our first experiments. The sensitivity to a thin layer is apparent when one realizes that the equilibrium shift in the binding curve in **Figure 1a,c** is for a layer only 0.3 nm thick. The relatively large spectral shift in comparison with the linewidth in this case (**Fig. 1a**) reveals the ease with which the binding of this layer can be detected.

The sensitivity for molecules binding on the equator, where the principle photon energy circulates, is theorized to be much greater than the surface-averaged sensitivity and increases more favorably as the radius is reduced ( $\Delta\lambda_r/\lambda_r \propto R^{-5/2}$ )<sup>4</sup>. We projected that one virion having one-tenth the mass of HIV could be easily detected by working at shorter wavelengths where  $Q$  is considerably increased because of lower water absorption and by reducing the radius of the microsphere to  $\sim 45$   $\mu\text{m}$ <sup>10</sup>. What we did not anticipate was that a simple nonlinear effect could improve on our sensitivity by orders of magnitude and turn the WGM biosensor into a *bona fide* sensor for a single unlabeled protein.

On a single-molecule level our effect works by polarizing each adsorbate in the evanescent field of the resonator—a simple ‘reactive’ effect<sup>4</sup>. Although we considered the refractive index of the microsphere to be constant, it actually does change in the process of molecules binding by the so-called ‘thermo-optic’ effect. If sufficient intensity resides in the evanescent field, then a non-negligible heating of the bound molecule occurs, which in turn transfers heat to the silica. This raises the temperature locally, which raises the refractive index because of silica’s positive thermo-optic coefficient,  $dn/dT$ . Consequently, an additional wavelength shift occurs. The more power circulates in the resonator, the larger the thermo-optic shift. A greater circulating power can build up in a WGM resonator having a larger  $Q$ . A group led by Vahala<sup>5</sup> managed to circulate  $\sim 100$  Watts in their resonator with only 1 mW of laser power, by using a

micro-toroid resonator with a  $Q$  of  $2 \times 10^8$ . In addition to generating a larger shift for a single binding event, their shift sensitivity also increased by virtue of having a narrower linewidth. Binding of protein led to reported steps in wavelength shift data (similar to that shown the insert in **Fig. 1c**)

### Current implementations and applications

In pilot experiments, we have demonstrated the quantitative use of the WGM microsphere biosensor for detection of protein<sup>3,4</sup>, DNA and a single-nucleotide polymorphism<sup>9</sup>. In these demonstrations, we functionalized the silica surface of the microsphere with biological recognition elements: we immobilized antibodies as well as other molecules for specific detection of proteins and conjugated oligonucleotides to dextran hydrogels for sensitive DNA and single-nucleotide polymorphism analysis by hybridization. An initial sensitivity of  $\sim 1$  pg/mm<sup>2</sup> for label-free detection of biomolecules was unprecedented and prompted different research efforts using our approach.

The broad interest in the technique rests in part on the fact that WGMs can be excited in various cavity geometries and materials (**Fig. 3**). For example, the cross-section of the microsphere in **Figure 1b** along the equator resembles a disk, and it is indeed possible to launch WGMs in disk or ring-shaped resonators fabricated on planar substrates. Such chip-based platforms have an important advantage: devices can be manufactured by means of standard photolithography techniques<sup>11–14</sup> for which various transparent materials can be used. In this respect, the possibility of using polymer thin films for fabrication of high- $Q$  disk or ring resonators<sup>11,15</sup> can offer an advantage by providing alternative surface chemistry for conjugation to biomolecules. Planar resonators can also facilitate the integration with soft lithography-based microfluidics<sup>16</sup> as the substrate can be directly bonded to slabs of replica-molded channel structures—an effort already ongoing for the more challenging microsphere geometry<sup>10,17</sup>. Alternatively, a glass capillary in which resonance is excited along its perimeter can act as an elegantly conceived WGM sensor with an already integrated microfluidic channel<sup>18</sup>.

In all these diverse implementations, the WGMs allow us to obtain quantitative information about molecules and their interactions. Owing to their spherical symmetry, microsphere-based sensors are amenable to rigorous theoretical analysis using Maxwell’s equations, and a simple formula can be derived that relates the resonance shift to surface density of bound molecules and their polarizability<sup>4,19</sup> (**Box 1**). For other cavity geometries, theoretical analysis can be approximated by use of finite element simulations<sup>20</sup> or mathematical resonator models<sup>21</sup>. In the limit of single-molecule detection, the magnitude of a ‘reactive’ wavelength shift can in principle be used to estimate the molecular weight of a protein (or DNA) molecule as its polarizability is proportional to the number of amino acids (or nucleotides).

Additional modification of the WGM technique quickly took applications beyond the initial proposal of a simple, ultrasensitive and label-free biosensor. For example, WGMs can be excited with an electromagnetic field polarized tangent (**Fig. 1**) or perpendicular (**Fig. 2**) to the resonator surface, and this polarization versatility can be used to measure the anisotropy in the refractive index of an adsorbed layer. On a molecular level this anisotropy exists because molecules self-assemble in preferred orientations. By comparing the measured ratio of the shift of the tangentially polarized WGM to the shift of the perpendicularly polarized WGM with theory, this preferred orientation can be determined.

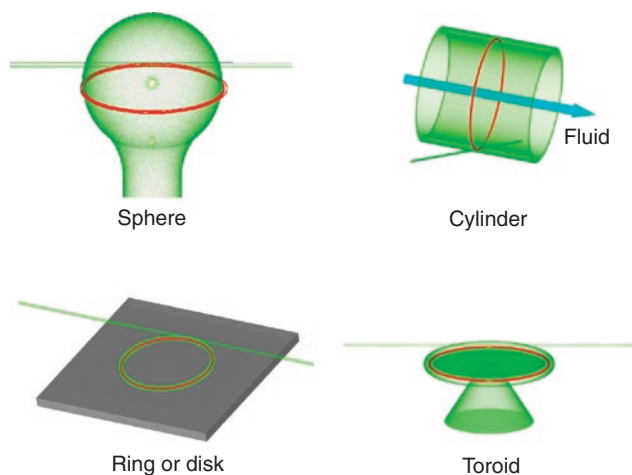


**Figure 3** | WGM resonator geometries. The WGM is highlighted in red, blue indicates microfluidic flow.

The polarization-sensing technique has already not only been used for static anisotropy measurements<sup>22</sup> but also to follow conformational changes in self-assembled monolayers such as biological membranes<sup>23</sup>. Extension of this approach might allow screening for agonists that induce functionally relevant conformations in G protein-coupled receptors<sup>24</sup>, one of the largest families of drug targets. Measurements at two polarizations can also benefit from operation at several wavelengths, for example, in pump-probe spectroscopy. Here a WGM (pump) induces conformational and other structural changes in a photosensitive molecule that are measured simultaneously from the shift of a second WGM (probe) at a wavelength that does not interfere with stimulation by the pump. This approach has been demonstrated for measurements of conformational changes associated with photoinduced isomerization of retinal in a bacteriorhodopsin membrane<sup>23</sup>. We believe that the approach can be extended, for example, to study structural changes coupled to photoinduced charge separation in photosynthetic membranes<sup>25</sup>.

Optical microcavities also provide a useful tool to study biologically important surface coatings and aggregates that are formed from larger particles such as micrometer-sized cells and bacteria. Analytic equations were derived for microsphere sensors that relate wavelength shift to bacterial surface density<sup>26</sup>. Predictions were confirmed in measurements taken with *Escherichia coli* as a model system, establishing WGM biosensors as a sensitive technique for detection and analysis of microorganisms<sup>26</sup>.

In other applications it was shown that particles such as virions do not need to bind to the resonator surface to induce a wavelength shift. For such larger particles, random walk resulting from Brownian motion within the evanescent field leads to resonance wavelength fluctuations. The autocorrelation of this signal allows the size of these particles to be estimated<sup>17</sup> in a label-free approach reminiscent of fluorescence-correlation spectroscopy. The above examples illustrate the use of WGM sensors for a wide variety of analyses that include biomolecules and their interactions as well as virions<sup>10</sup>, cells and bacteria (Fig. 4).

### Future outlook

Although experiments with prototypes have demonstrated the large potential of the WGM technique, there is still plenty of room for improvement. Multiple sensors integrated in a lab-on-a-chip could provide rapid information on the chemical composition of a blood sample or could be used to map the affinity of a library of small organic molecules binding to target receptors. Multiplexed high-throughput WGM devices may also advance progress in proteomics and genomics where large sampling rates are required to understand the complete network of biomolecular interactions that have evolved in the cell. It is therefore desirable to fabricate the next generation of sensors in an array format, possibly by using replica molding<sup>27</sup> or photolithography<sup>28</sup>. Photolithographic techniques are well established for processing of silicon material, and sensors that are made from silicon and operate in the transparent telecom band (1,310/1,550 nm) could exploit the possibility of further integration with state-of-the-art electronic and photonic circuits. In this respect, photonic crystal (nano)cavities may provide an alternative cavity geometry that combines a high-Q factor with ultra-small size on a planar silicon substrate<sup>29,30</sup>. Miniaturization of microcavities seems promising by use of transparent high-refractive-index materials (such as silicon, doped glasses or sapphire) as the wavelength within a WGM is scaled down. Miniature microsphere or photonic

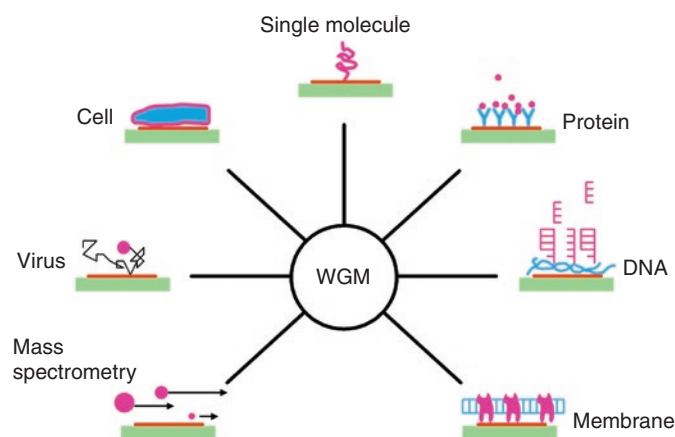


**Figure 4** | Applications of WGM biosensors for analysis of various biological materials in different configurations.

crystal sensors with footprints of only several square micrometers are conceivable and could be encapsulated in lipid vesicles or empty red blood cells. Masked by an inert membrane, these sensors could evade the immune system and circulate throughout the cardiovascular system probing for toxins or disease markers that diffuse to the detector through deliberately engineered membrane pores. In this case, the WGM could be read out noninvasively by collecting the scattered light after excitation with a near-infrared laser<sup>31</sup> focused through the skin or through more transparent body segments such as the eye. For this idea to work it will be necessary to develop efficient schemes to couple to the free-space beam.

The ability of the WGM sensor to probe molecules close to the sensing surface without the need for binding<sup>17</sup> may be exploited in applications that sample analyte during its time of passage through that sensitive volume. Such an ‘optical mass spectrometer’ could use microfluidic flow to direct the analyte molecules past the WGM resonator for rapid profiling of mass distribution and concentration. Alternatively, measurements that use electrophoretic induced flow could be used to determine mobility of an analyte. Such applications will rely on the high speed of the detection mechanism, which is limited for WGM by the photon lifetime:  $\tau = Q/\omega_r$ , typically on the order of nanoseconds (with  $\omega_r$  being the resonance frequency).

As the first all-optical label-free single-molecule technique, the WGM platform promises unprecedented insights in the non-equilibrium dynamics of molecular recognition, conformational changes and biomolecular function. Optical resonators can be modified and combined with other optical techniques, for example, to measure the spectroscopic fingerprint of a bound analyte. In this case, the local field intensity of a WGM can be additionally amplified by excitation of surface-plasmon resonance in immobilized gold or silver nanoparticles. Ideally, the field intensities are large enough so that surface-enhanced Raman spectroscopy of a few molecules bound to the metal particle will become feasible by using a state-of-the-art monochromator to analyze the scattered light<sup>32</sup>.

Other than for analysis of biomolecules, the WGM sensor can be used in cell-based assays. WGM sensor response is local to the membrane of a cell directly immobilized on the resonator surface, which can be used to determine dynamic mass redistribution that occurs during the signaling event of a membrane receptor, for example, in response to a growth hormone<sup>33,34</sup>. The kinetic fingerprint of such

signaling events can be associated with certain biochemical pathways, which could aid in finding drugs with fewer side effects or in mapping signaling pathways.

The above examples highlight some of the exciting future applications that we envision for WGM biosensors. Possible applications can be extended to, for example, high-sensitivity detection of disease markers in point-of-care testing, high-throughput screening of lead compounds in drug discovery as well as basic research studies in various disciplines within the life sciences such as signal transduction, protein folding and membrane biophysics. With prospects of such a bright future, we are confident that optical resonators will make grand contributions for improved health care, novel biomedical applications and for development of state-of-the-art tools in the life sciences.

#### ACKNOWLEDGMENTS

S.A. was supported by the US National Science Foundation grant BES-0522668, and F.V. was supported by a Rowland Junior Fellowship.

Published online at <http://www.nature.com/naturemethods/>.

Reprints and permissions information is available online at <http://npg.nature.com/reprintsandpermissions/>.

- Cooper, M.A. Label-free screening of bio-molecular interactions. *Anal. Bioanal. Chem.* **377**, 834–842 (2003).
- Nakatani, K., Sando, S. & Saito, I. Scanning of guanine-guanine mismatches in DNA by synthetic ligands using surface plasmon resonance. *Nat. Biotechnol.* **19**, 51–55 (2001).
- Vollmer, F. *et al.* Protein detection by optical shift of a resonant microcavity. *Appl. Phys. Lett.* **80**, 4057–4059 (2002).
- Arnold, S., Khoshima, M., Teraoka, I., Holler, S. & Vollmer, F. Shift of whispering gallery modes in microspheres by protein adsorption. *Opt. Lett.* **28**, 272–274 (2003).
- Armani, A.M., Kulkarni, R.P., Fraser, S.E., Flagan, R.C. & Vahala, K.J. Label-free, single-molecule detection with optical microcavities. *Science* **317**, 783–787 (2007).
- Serpengüzel, A., Arnold, S. & Griffl, G. Excitation of resonances of a microsphere on an optical fiber. *Opt. Lett.* **20**, 654–656 (1995).
- Knight, J.C. & Cheung, G., Jacques, F. & Birks, T.A. Phase-matched excitation of whispering-gallery-mode resonances by a fiber taper. *Opt. Lett.* **22**, 1129–1131 (1997).
- Griffl, G. *et al.* Morphology-dependent resonances of a microsphere-optical fiber system. *Opt. Lett.* **21**, 695–697 (1996).
- Vollmer, F., Arnold, S., Braun, D., Teraoka, I. & Libchaber, A. Multiplexed DNA quantification by spectroscopic shift of two microsphere cavities. *Biophys. J.* **85**, 1974–1979 (2003).
- Arnold, S., Ramjit, R., Keng, D., Kolchenko, V. & Teraoka, I. Microparticle photophysics illuminates viral biosensing. *Faraday Discuss.* **137**, 65–83 (2008).
- Chao, C.Y. & Guo, L.J. Polymer microring resonators for biochemical sensing applications. *IEEE J. Selected Topics Quantum Electron.* **12**, 134–142 (2006).
- Zhu, H.Y., White, I.M., Suter, J.D., Suter, P.S. & Fan, X.D. Analysis of biomolecule detection with optofluidic ring resonator sensors. *Opt. Express* **15**, 9129–9146 (2007).
- De Vos, K., Bartolozzi, I., Schacht, E., Bienstman, P. & Baets, R. Silicon-on-insulator microring resonator for sensitive and label-free biosensing. *Opt. Express* **15**, 7610–7615 (2007).
- Yalcin, A. *et al.* Optical sensing of biomolecules using microring resonators. *IEEE Journal of Selected Topics in Quantum Electronics* **12**, 148–155 (2006).
- Rabiei, P., Steier, W.H., Zhang, C. & Dalton, L.R. Polymer micro-ring filters and modulators. *J. Lightwave Technol.* **20**, 1968–1974 (2002).
- McDonald, J.C. *et al.* Fabrication of microfluidic systems in poly(dimethylsiloxane). *Electrophoresis* **21**, 27–40 (2000).
- Keng, D., McAnanama, S.R., Teraoka, I. & Arnold, S. Resonance fluctuations of a whispering gallery mode biosensor by particles undergoing Brownian motion. *Appl. Phys. Lett.* **91**, 103902 (2007).
- White, I.M., Oveys, H., Fan, X., Smith, T.L. & Zhang, J. Integrated multiplexed biosensors based on liquid core optical ring resonators and anti-resonant reflecting optical waveguide. *Appl. Phys. Lett.* **89**, 191106 (2006).
- Teraoka, I., Arnold, S. & Vollmer, F. Perturbation approach to shift of whispering-gallery modes in microspheres by protein adsorption. *J. Opt. Soc. Am. B* **20**, 1937–1946 (2003).
- Quan, H.Y. & Guo, Z.X. Simulation of whispering-gallery-mode resonance shifts for optical miniature biosensors. *J. Quant. Spectrosc. Radiat. Transf.* **93**, 231–243 (2005).
- Boyd, R.W. & Heebner, J.E. Sensitive disk resonator photonic biosensor. *Appl. Opt.* **40**, 5742–5747 (2001).
- Noto, M., Keng, D., Teraoka, I. & Arnold, S. Detection of protein orientation on the silica microsphere surface using transverse electric/transverse magnetic whispering gallery modes. *Biophys. J.* **92**, 4466–4472 (2007).
- Topolancik, J. & Vollmer, F. Photoinduced transformations in bacteriorhodopsin membrane monitored with optical microcavities. *Biophys. J.* **92**, 2223–2229 (2007).
- Hoffmann, C., Zuern, A., Buenemann, M. & Lohse, M.J. Conformational changes in G-protein-coupled receptors—the quest for functionally selective conformations is open. *Br. J. Pharmacol.* **153**, S358–S366 (2008).
- Gust, D., Moore, T.A. & Moore, A.L. Mimicking photosynthetic solar energy transduction. *Acc. Chem. Res.* **34**, 40–48 (2001).
- Ren, H.-C., Vollmer, F., Arnold, S. & Libchaber, A. High-Q microsphere biosensor—analysis for adsorption of rodlike bacteria. *Opt. Express* **25**, 17410–17423 (2007).
- Armani, A.M., Srinivasan, A. & Vahala, K.J. Soft lithographic fabrication of high Q polymer microcavity arrays. *Nano Lett.* **7**, 1823–1826 (2007).
- Boyd, R.W. *et al.* Nanofabrication of optical structures and devices for photonics and biophotonics. *J. Mod. Opt.* **50**, 2543–2550 (2003).
- Lee, M. & Fauchet, P.M. Two-dimensional silicon photonic crystal based biosensing platform for protein detection. *Opt. Express* **15**, 4530–4535 (2007).
- Skivesen, N. *et al.* Photonic-crystal waveguide biosensor. *Opt. Express* **15**, 3169–3176 (2007).
- Poon, A.W., Chang, R.K. & Chowdhury, D.Q. Measurement of fiber-cladding diameter uniformity by use of whispering-gallery modes: nanometer resolution in diameter variations along millimeter to centimeter lengths. *Opt. Lett.* **26**, 1867–1869 (2001).
- White, I.M., Gohring, J. & Fan, X. SERS-based detection in an optofluidic ring resonator platform. *Opt. Express* **25**, 17433–17442 (2007).
- Fang, Y., Ferrie, A., Fontaine, N. & Yuen, P. Characteristics of dynamic mass redistribution of EGF receptor signaling in living cells measured with label-free optical biosensors. *Anal. Chem.* **77**, 5720–5725 (2005).
- Fang, Y., Ferrie, A., Fontaine, N., Mauro, J. & Balakrishnan, J. Resonant waveguide grating biosensor for living cell sensing. *Biophys. J.* **91**, 1925–1940 (2006).
- Arnold, S. Microspheres, photonic atoms, and the physics of nothing. *Am. Sci.* **89**, 414–421 (2001).